



Identification of a combined lncRNA prognostic signature and knockdown of lncRNA MANCR to inhibit progression of clear cell renal cell carcinoma by bioinformatics analysis

Sheng Xue^{1#}, Hanxu Guo^{2#}, Shibo Wei³, Yuan Song¹, Junfeng Huang¹, Shuo Deng¹, Qingwen Li¹, Wenyong Li¹

¹Department of Urology, The First Affiliated Hospital of Bengbu Medical College, Bengbu, China; ²School of Clinical Medicine, Bengbu Medical College, Bengbu, China; ³School of Anesthesiology, Bengbu Medical College, Bengbu, China

Contributions: (I) Conception and design: S Xue, W Li; (II) Administrative support: Q Li; (III) Provision of study materials or patients: S Xue, H Guo, W Li; (IV) Collection and assembly of data: S Wei, Y Song, J Huang, S Deng; (V) Data analysis and interpretation: S Xue, H Guo; (VI) Manuscript writing: All authors; (VII) Final approval of manuscript: All authors.

[#]These authors contributed equally to this work.

Correspondence to: Qingwen Li; Wenyong Li. Department of Urology, The First Affiliated Hospital of Bengbu Medical College, 287 Changhuai Road, Bengbu 233004, China. Email: bbmclqw537@163.com; 1435113472@qq.com.

Background: Long non-coding RNAs (lncRNAs) have become potential therapeutic targets or promising prognostic biomarkers in cancers. However, individual gene does not show sufficient prognostic value for clear cell renal cell carcinoma (ccRCC). Therefore, this study aims to develop a combined prognostic lncRNA signature to the prognosis of ccRCC.

Methods: The transcriptome profiling data for confirmed ccRCC cases were obtained from The Cancer Genome Atlas (TCGA; <https://portal.gdc.cancer.gov/>). The prognostic significance, survival time and diagnostic effectiveness of the lncRNAs in ccRCC was evaluated using Kaplan-Meier method, the log-rank test and receiver operating characteristic (ROC) curves, respectively. The area under the ROC curve (AUC) of the 4 lncRNAs was also performed. The expression of mitotically-associated lncRNA (MANCR) was measured in ccRCC cells or tissues by reverse transcription quantitative polymerase chain reaction (RT-qPCR). Both Colony formation assays and Cell Counting Kit-8 (CCK-8) assay was conducted to detect the proliferation of both 786-O and SN12C cells. For apoptosis detection, flow cytometry in both 786-O and SN12C cells was performed. For migration of 786-O and SN12C cells detection, wound healing and transwell assays were performed.

Results: A total of 1,567 differentially expressed lncRNAs in ccRCC were discerned with 1,340 upregulation and 227 downregulation. Furthermore, a 4-lncRNA signature (*FIRRE*, *MANCR*, *AC103706.1*, and *AC018648.1*) model was obtained that showed good performance in the prognosis of ccRCC. Gene Ontology (GO) analysis showed that these protein-coding genes (PCGs) were mainly enriched in ATPase activity, catalytic activity, and acting on RNA protein serine/threonine kinase activity. Kyoto Encyclopedia of Genes and Genomes (KEGG) pathway analysis showed that PCGs were mainly involved in endocytosis, oocyte meiosis and spliceosome. In addition, we revealed that *MANCR* was highly expressed in ccRCC cells and tissues and downregulation of *MANCR* inhibited cell proliferation and migration. In contrast, apoptosis of 786-O and SN12C cells was promoted with *MANCR* suppression.

Conclusions: A 4-lncRNA prognostic model that presented good performance for prognosis of ccRCC patients was established. Knockdown of *MANCR* inhibited cell proliferation and migration, and promoted apoptosis of 786-O and SN12C cells, suggesting that a 4-lncRNA signature model might be an essential for ccRCC prognosis.

Keywords: Clear cell renal cell carcinoma (ccRCC); mitotically-associated lncRNA (MANCR); prognosis

Submitted Jul 05, 2022. Accepted for publication Sep 06, 2022.

doi: 10.21037/tau-22-527

View this article at: <https://dx.doi.org/10.21037/tau-22-527>

Introduction

Clear cell renal cell carcinoma (ccRCC) is the second most common cancer of the urinary system after bladder cancer. It is the most common type which accounts for about 80% of renal cancer (1). In recent years, the incidence of ccRCC is increasing every year. It has been proved that ccRCC was usually insensitive to radiotherapy, chemotherapy, and immunotherapy. So far, surgery is the main treatment method for ccRCC (2). Around 60% of patients with ccRCC die within 1–2 years after diagnosis, and 30% of patients with ccRCC have developed distant metastasis by the time of diagnosis (3). Therefore, it is urgent to explore the novel effective biomarkers for the prognosis of ccRCC. At present, with the continuous understanding of the pathogenesis of ccRCC, important progresses have been made in the research of various molecular markers related to ccRCC prognosis, such as ferroptosis-related gene CHAC1, autophagy-related gene P4HB and glycolysis-related genes (4–6). However, these markers performed poorly in ccRCC prognosis. Therefore, biomarkers of prognosis evaluation for ccRCC patients deserved deep study.

Long non-coding RNAs (lncRNAs) belongs to functional RNA molecules and the length of lncRNAs usually is more than 200 nucleotides. lncRNAs are important epigenetic regulators that control gene expression and affect diverse biological processes (7). They can participate in cell differentiation, growth development, stress response, disease development, and other biological processes via epigenetic regulation and biological information exchange. Studies have proved that lncRNAs are important molecular players in the regulation of various types of cancer progression (8), including that of ccRCC. An increasing number of studies have confirmed that abnormal expression of lncRNAs promoted or inhibited ccRCC development via regulating the proliferation, invasion, and migration of ccRCC. Such as, *lncRNA DNAJC3-AS1* promoted ccRCC development via downregulating PRDM14 expression by sponging miR-27a-3p (9); *lncRNA LINC00973* inhibited cancer immune via promoting the expression of Siglec-15 in ccRCC (10); and *lncRNA SNHG16* decreased *CDKN1A* expression which will promote ccRCC development by regulating cell migration and invasion of ccRCC (11).

These findings revealed that lncRNA plays crucial role in the progression of ccRCC. In fact, lncRNAs have been showed more potential prognostic value in different cancers owing to its widely regulation ability. Several lncRNAs have also been considered important prognostic parameters in ccRCC, such as *lncRNA Fer1LA*, *LINC00460*, and *LncRNA SNHG17* (12–14). However, most of the members in the huge family of lncRNAs have not yet been studied. Therefore, it is necessary to identify more lncRNAs and clarify the function of lncRNAs to improve the prognostic assessment system of ccRCC. Recently, several prognostic model of lncRNA signature in ccRCC have been studied and the combined signature showed better performance in prognosis of ccRCC (15–17). Therefore, it will help to better perform prognostic assessment and precise treatment of ccRCC to screen key differentially expressed lncRNAs with a combined prognostic model.

In the present study, differentially expressed lncRNAs were excavated and identified using The Cancer Genome Atlas (TCGA) high-throughput database data and a key ccRCC prognostic lncRNA signature was constructed, and the function of the key lncRNA in ccRCC was detected. We aimed to explore the useful lncRNA model for clinical judgment of ccRCC prognosis, and to supply new ideas for the research into the etiology and pathogenesis of ccRCC. We present the following article in accordance with the MDAR reporting checklist (available at <https://tau.amegroups.com/article/view/10.21037/tau-22-527/rc>).

Methods

In the present study, combined lncRNAs signature used for prognosis of ccRCC was established by bioinformatics analysis using the transcriptome profiling data from TCGA database. A 4-lncRNA signature (*FIRRE*, *MANCR*, *AC103706.1*, and *AC018648.1*) model with an area under the curve (AUC) value of 0.711 was obtained that showed good performance in the prognosis of ccRCC. Gene Ontology (GO) and Kyoto Encyclopedia of Genes and Genomes (KEGG) assays were used to identify the pathways protein-coding genes (PCGs) involved in. The function of the key lncRNA *MANCR* from the combined

lncRNAs signature was evaluated by downregulation of lncRNA *MANCR* in 786-O and SN12C cells.

Data acquisition and processing

Expression profiles of messenger RNA (mRNA) and lncRNAs of ccRCC were downloaded from The Cancer Genome Atlas (TCGA) database (<https://portal.gdc.cancer.gov/>). The expression of mRNA and lncRNAs was analyzed by EdgeR on a HT-Seq platform, including 539 ccRCC tissues and 72 adjacent normal tissues. Matched clinical data from ccRCC patients were also downloaded from TCGA database. In the cohort, 611 patients were included, among whom 602 had intact survival data recorded. The clinicopathological indicators including stage (stage I–IV), pathologic_T (T1–T4), pathologic_N (N0–N3) and pathologic_M (M0–M3).

According to the annotation of the expression profiles from the National Center for Biotechnology Information (NCBI; <https://www.ncbi.nlm.nih.gov/>) and Ensembl (<https://asia.ensembl.org/index.html>) databases, 33,800 mRNA and 14,142 lncRNAs were identified. For the differential expression of lncRNAs assay, a R language package DESeq was performed. And the parameter as follows: adjusted $P < 0.05$ and absolute \log_2 (Fold Change) > 1 . The lncRNAs with fold changes (FC) less than 1 were excluded. R Cluster Profiler package was used to conduct the GO and KEGG functional enrichment. The study was conducted in accordance with the Declaration of Helsinki (as revised in 2013).

Cox proportional hazards model

In order to pair the differentially expressed genes (DEGs) with survival data, the correlation analysis was performed based on the relevant clinical data from TCGA-kidney renal clear cell carcinoma (KIRC) database with a univariate Cox proportional hazards model. Briefly, the combined cases were input into the model and the P value was obtained. Then, based on the ranking of the P value, the top 4 lncRNAs were selected for further analysis. The hazard ratio (HR) was calculated in each significant lncRNA. The discrimination between real and prediction value was evaluated by the concordance index (C-index). The prognostic significance, survival time and diagnostic effectiveness of the lncRNAs in ccRCC was evaluated using Kaplan-Meier method, the log-rank test and receiver operating characteristic (ROC) curves, respectively. In

addition, the area under the ROC curve (AUC) of the 4 lncRNAs was also used to further analysis. To better show the cases of ccRCC that are matched with lncRNAs, the risk curve, heatmap, and survival status figures were conducted.

Co-expression of lncRNA predictive target genes

In order to evaluate the co-expression relationships between the lncRNAs and PCGs, the Pearson correlation coefficient between the expression profiles of lncRNAs and PCGs was calculated. A Pearson correlation coefficient > 0.40 indicated lncRNA-related PCGs.

Cell lines, culture, and transfection

The human ccRCC cell lines were purchased from the Procell Life Science&Technology Co., Ltd, including A498, ACHN, SN12C, 786-O, and 769-P. These cells were recovered, passaged and then cultured in Dulbecco's modified Eagle medium (DMEM; Corning, Corning, NY, USA, R10-017-CV) containing 10% fetal bovine serum (FBS; Invitrogen, Carlsbad, CA, USA, 16000-044) and penicillin-streptomycin (Gibco, Grand Island, NY, USA, 15140122) in a humidified 5% CO_2 atmosphere at 37 °C. For cell transfection, 2×10^5 cells/well 786-O and SN12C cells were plated 6-well plates and cultured for 24 hours at 37 °C until the cell confluence reached at 70–90%. The cells were then transfected with lentivirus containing the short hairpin RNA (shRNA) of mitotically-associated lncRNA (*MANCR*) and the following experiments were conducted at 48 hours after transfection. The lentivirus containing shRNA of *MANCR* was purchased from Shanghai Yibeirui Biomedical Science and Technology Co., Ltd. The sequence of shRNA of *MANCR* as follows: (SH-114)-KD-1: GGAGATAGAGCACAGCCAT; (SH-114)-KD-2: GCTTGCTCTCACAGCCATT; (SH-114)-KD-3: CCGAGTGGCACTCATACAT.

Total RNA extraction and quantitative real-time polymerase chain reaction (qRT-PCR)

Total RNA from the ccRCC cell lines with different treatment was extracted using TRIzol reagent (Sigma Aldrich, St. Louis, MO, USA, T9424-100 mL). Subsequently, complementary DNA (cDNA) was obtained by reverse transcription with 800 ng RNA using a commercial kit Hiscript QRT supermix for qPCR (+gDNA WIPER) (Vazyme,

Beijing, China, R123-01). The relative expression of MANCR was performed in an ABI7500 instrument (Applied Biosystems, Waltham, MA, USA) using AceQ qPCR SYBR Green master mix (Vazyme, Beijing, China, Q111-02). The relative expression of MANCR was calculated by $2^{-\Delta\Delta C_t}$ method with Glyceraldehyde 3-phosphate dehydrogenase (GAPDH) as the internal control. The primer sequences used for qRT-PCR were as follows: GAPDH, Forward: 5'-TGACTTCAACAGCGACACCCA-3', Reverse: 5'-CACCTGTGCTGTAGCCAAA-3' (antisense); and lncMANCR, Forward: 5'-TTGGGAGGCTGAGTCTAAGTGT-3', Reverse: 5'-GCGAGTGGTGAGTGGA TGTG-3'.

Cell proliferation assay

Cell Counting Kit-8 (CCK-8; Dojindo, Kumamoto, Japan, ck04) was used to detect the cell proliferation with different treatment. Briefly, 100 μ L cells (2,000 cells/well) were seeded in 96-well plates and then cells were incubated at 37 °C in a humidified 5% CO₂ atmosphere for 0, 24, 48, and 72 hours, respectively. Subsequently, the wells were added with 10 μ L of CCK-8 and incubated for 2 hours. The absorbance was measured by a microplate reader at 450 nm.

Colony formation assay

786-O and SN12C cells (500 cells per well) were seeded in 6-well plates and cultured at 37 °C in a humidified 5% CO₂ atmosphere. The cells were harvested and fixed with 100% methanol after incubation for 14 days. Then, 0.1% (w/v) crystal violet was used to stain the cells and photographed with a microscope (CX41, Olympus) in bright field.

Wound healing assay

The 786-O and SN12C cells were cultured in DMEM (Corning, R10-017-CV) containing 10% FBS (Invitrogen, 16000-044). Then, the 786-O and SN12C cells were trypsinized in the logarithmic growth phase and resuspended in the complete medium. Subsequently, the cells (50,000 cells/well) were seeded in a 96-well plate and were incubated at 37 °C in a 5% CO₂ incubator with a culture system of 100 μ L/well. A scratch instrument was used to form a scratch at the lower center of the 96-well plate. Then, the serum-free medium was used to rinse the cells for 2–3 times. A low concentration serum (0.5%)

medium was added and the cells were photographed at 0 hour. Subsequently, the cells were incubated at 37 °C in a 5% CO₂ incubator for 12 hours. The migration of cells was scanned and the migration area was screened using cellomics (Thermo Fisher, Waltham, MA, USA).

Transwell assay

Transwell assay was also used to detect cell migration. Briefly, the chamber was placed in a 24-well plate with 100 μ L of serum-free medium and placed in the incubator for 1–2 hours. Then, 786-O and SN12C cells were seeded in the upper chambers of a transwell (Corning) without serum. Medium containing 30% FBS was placed in the lower chambers. Cells were stained with 400 μ L crystal violet for 5 minutes after incubation at 37 °C in a 5% CO₂ incubator for 24 hours. Finally, the images of the migrated cells were taken using an optical microscope.

Flow cytometry analysis of apoptosis

The apoptosis rates of 786-O and SN12C cells were detected by flow cytometry using Annexin V-APC and PI Kit (SouthernBiotech, Birmingham, AL, USA, 10010-09). Briefly, the 786-O and SN12C cells were collected and then washed 2 times with phosphate buffer saline (PBS). Then, 5 μ L annexin V-APC and 5 μ L propidium iodide (PI) was used to stain the cells for 15 minutes. The cells were then resuspended to 1 mL with 1 \times apoptosis buffer after staining. Finally, 200 μ L of cell suspension was added to the 96-well plate (3 duplicate wells in each group) and then transferred to a flow cytometer tube. The apoptosis of flow cytometry was detected by high-throughput flow cytometry (Millipore, Burlington, MA, USA, Guava easyCyte 6HT-2L).

Statistical analysis

Statistical analysis in the preset study was analyzed using the software GraphPad Prism 7.0 (GraphPad, San Diego, CA, USA) and SPSS 21.0 (IBM Corp., Armonk, NY, USA) with at least 3 biological repetitions in this study. AUC \geq 0.7 indicated a good prognosis prediction for the prognostic model. This study aims to investigate the differentially expressed lncRNAs in ccRCC and established the combined lncRNAs prognosis prediction model. The training and validation samples for the development and validation of the lncRNAs based prognosis prediction model will be

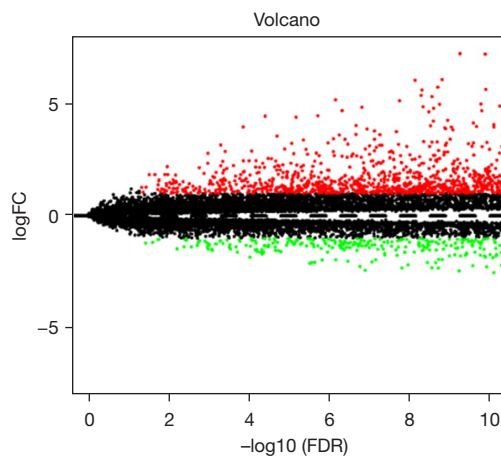


Figure 1 Differentially expressed lncRNA identification in ccRCC from TCGA. The volcano plot of the differentially expressed lncRNA from the transcriptome profiling data was downloaded from TCGA database, included 539 ccRCC tissues and 72 adjacent noncancerous renal tissues. Red, green, and black dots indicated significantly upregulated-, downregulated- and non-differentially expressed lncRNAs, respectively. lncRNA, long non-coding RNA; ccRCC, clear cell renal cell carcinoma; TCGA, The Cancer Genome Atlas; FC, fold change; FDR, false discovery rate.

studies in the future study. Student's *t*-test was performed to analyze the differences between two groups. With two-tailed P value <0.05 was defined as statistically significant.

Results

Differentially expressed lncRNA identification in ccRCC from TCGA

In order to explore the differentially expressed lncRNAs in ccRCC, the transcriptome profiling data was downloaded from TCGA database and included 539 ccRCC tissues and 72 adjacent noncancerous renal tissues. A total of 1,567 differentially expressed lncRNAs in ccRCC were discerned with upregulation and 227 downregulation (Figure 1). Subsequently, *FIRRE*, *MANCR*, *AC103706.1*, and *AC018648.1* were entered into the multivariate Cox proportional hazards model according to the ranking of the P value. RiskScore = (0.1744 × *FIRRE* expression value) + (0.2637 × *AC103706.1* expression value) + (0.1869 × *AC018648.1* expression value) + (0.1274 × *MANCR* expression value). All of them showed high-risk features, suggesting that high expression indicated that the shortened

overall survival (OS) of patients. The C-index was 0.70 [95% confidence interval (CI): 0.66 to 0.74], which has significantly clinical value (P=5.44e-22). These results indicated that the *FIRRE*, *MANCR*, *AC103706.1*, and *AC018648.1* cluster showed important clinical prognostic value.

Evaluation of the prognostic model for the *FIRRE*, *MANCR*, *AC103706.1*, and *AC018648.1* cluster

Subsequently, the prognostic model of the *FIRRE*, *MANCR*, *AC103706.1*, and *AC018648.1* cluster was evaluated in 530 ccRCC patients. These patients were divided into low-risk (n=265) and high-risk (n=265) groups with 0.964 as the cut-off value based on the median RiskScore (Figure 2A). The survival status of 530 patients in the training cohort according to the 4-lncRNA signature risk score showed that high risk score indicated lower survival time (Figure 2B,2C). Kaplan-Meier OS curve in high-risk groups showed that the 3-year OS was 65.0% (95% CI: 59.1% to 71.5%) and the 5-year OS was 46.0% (95% CI: 39.2% to 54.1%). In low-risk ccRCC patients, 86.4% (95% CI: 81.9% to 91.1%) 3-year OS and 79.4% (95% CI: 73.7% to 85.6%) 5-year OS were observed, suggesting that the 3- and 5-year OS of low-risk ccRCC were dramatically higher compared with these high-risk ccRCC patients (Figure 2D). In addition, a better performance of AUC value with 0.711 was obtained based on the ROC curve for 4-lncRNA signature model (Figure 2E). These results indicated that the prognostic model for the *FIRRE*, *MANCR*, *AC103706.1*, and *AC018648.1* cluster showed good performance in the prognosis of ccRCC.

GO and KEGG enrichment analysis for PCGs co-expressed with 4 lncRNAs

To elucidate the pathways the *FIRRE*, *MANCR*, *AC103706.1*, and *AC018648.1* cluster is involved in, co-expression between the 4 lncRNAs and the PCGs was performed based on the Pearson correlation coefficients. A P value <0.05 was defined significantly associated with 4 lncRNAs. To further confirm the accurately prediction for the 4 lncRNAs model, GO and KEGG pathway enrichment were performed with 1,862 key PCGs (Pearson correlation coefficient >0.40 and P<1e-35). The GO analysis revealed that these PCGs were mainly enriched in ATPase activity and catalytic activity, and acting on RNA protein serine/threonine kinase activity

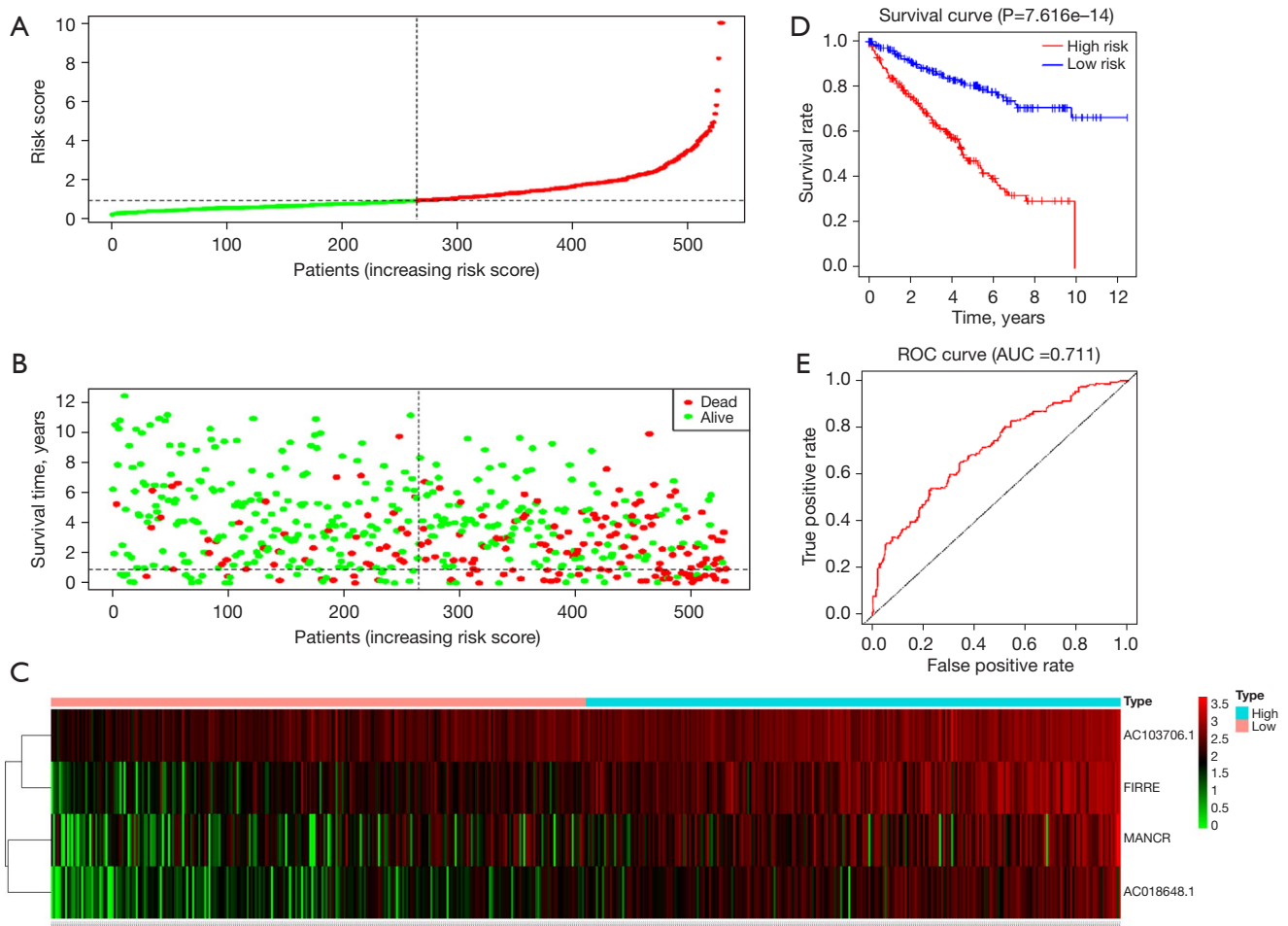


Figure 2 Evaluation of the prognostic model for the *FIRRE*, *MANCR*, *AC103706.1*, and *AC018648.1* cluster. (A) RiskScore of each ccRCC patient, low risk and high risk was indicated by green and red, respectively. (B) Survival time and status of each ccRCC patient with increasing risk score. (C) Heatmap for the expression of 4 lncRNAs in each ccRCC patient. Green to red indicated low to high expression level of lncRNAs. (D) Kaplan-Meier survival analysis was used to measure the survival rate with low-risk or high-risk patients. (E) ROC curve was used to predict survival with the AUC as 0.711. lncRNA, long non-coding RNA; ccRCC, clear cell renal cell carcinoma; ROC, receiver operating characteristic; AUC, the area under the ROC curve.

(Figure 3A). The KEGG pathway analysis indicated that the key PCGs were mainly involved in endocytosis, oocyte meiosis, spliceosome, carbon metabolism, and cell cycle (Figure 3B). These results revealed that the essential PCGs significantly related to 4 lncRNAs might be participated in ccRCC progression.

MANCR is highly expressed in ccRCC cells and tissues

To determine whether *MANCR* is involved in ccRCC development, *MANCR* expression was detected in ccRCC cells and tissues by RT-qPCR. The expression of *MANCR*

was firstly detected in several ccRCC cell lines, including A498, ACHN, SN12C, 786-O, and 769-P cells. The results indicated that *MANCR* was highly expressed in A498, ACHN, SN12C, 786-O, and 769-P cells, with the highest expression in SN12C cells (Figure 4A). The expression of *MANCR* detected in ccRCC tissues indicated that compared with adjacent tissues, *MANCR* expression was upregulated in 5 ccRCC tissues was significantly upregulated in 2 paired ccRCC tissues (Figure 4B) which was consistent with the transcriptome data. Furthermore, we demonstrated that high expression of *MANCR* is positively related to the stage and pathologic_T (Table 1). For survival curve analysis,

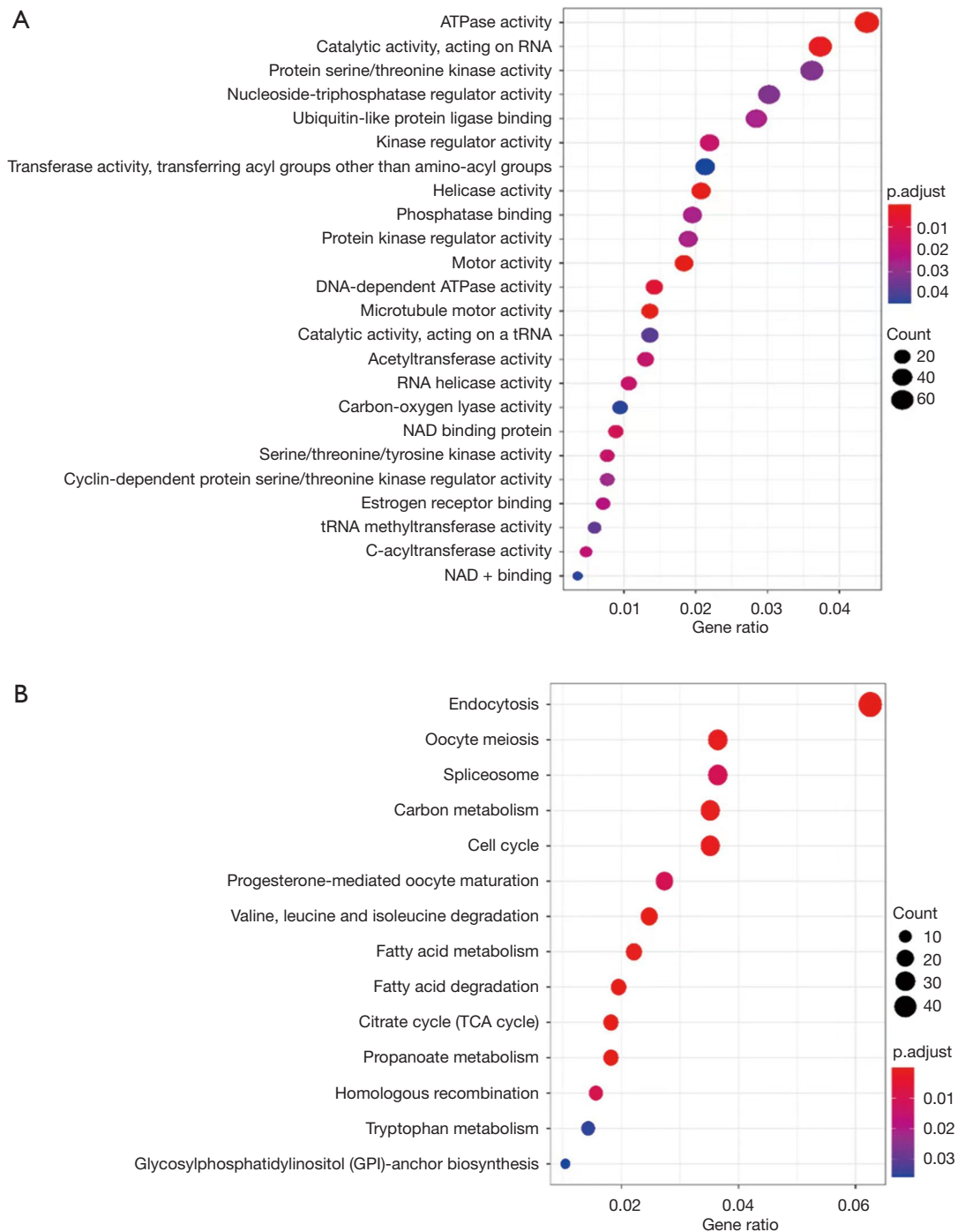


Figure 3 GO and KEGG enrichment analysis for PCGs co-expressed with 4 lncRNAs. (A,B) GO and KEGG enrichment analysis for PCGs which with four lncRNAs, respectively. 1,862 key PCGs meet to $|Pearson\ correlation\ coefficient| > 0.40$ and $P < 1e-35$ were selected. GO, Gene Ontology; KEGG, Kyoto Encyclopedia of Genes and Genomes; lncRNA, long non-coding RNA; PCG, protein-coding gene.

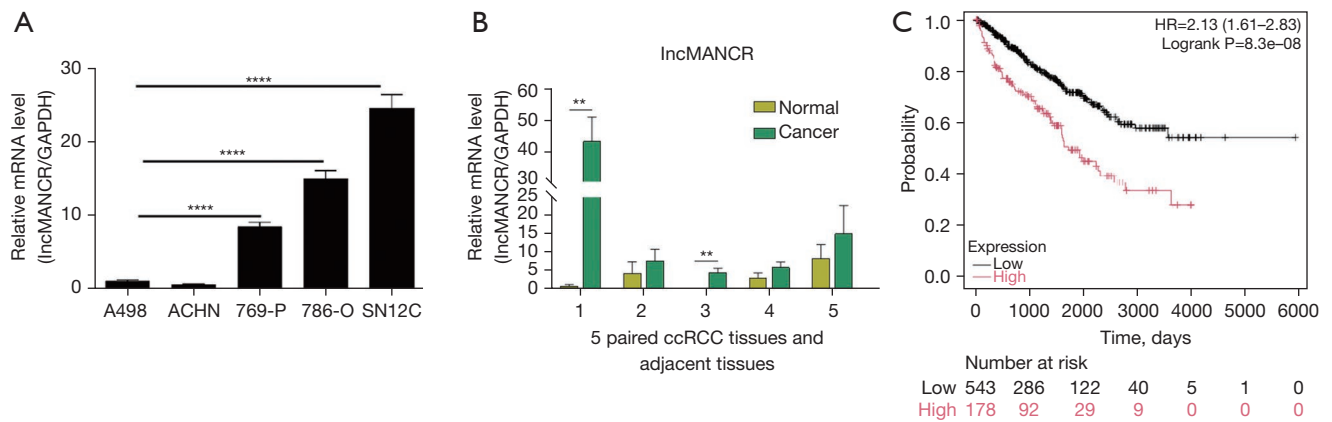


Figure 4 LncRNA MANCR is highly expressed in ccRCC cells and tissues. (A) The expression of *lncRNA MANCR* was detected in ccRCC cells by RT-qPCR, including A498, ACHN, SN12C, 786-O, and 769-P cells. (B) The expression of *MANCR* was detected by RT-qPCR in 5 paired ccRCC tissues and adjacent tissues, 1-5, 5 paired ccRCC tissues and adjacent tissues. (C) Survival curve analysis for *MANCR* expression in ccRCC patients. **, $P < 0.01$; ****, $P < 0.0001$. lncRNA, long non-coding RNA; RT-qPCR, reverse transcription quantitative polymerase chain reaction; ccRCC, clear cell renal cell carcinoma.

Table 1 The correlation between the expression of *MANCR* and clinicopathological indicators

| Characteristics | <i>MANCR</i> expression | | Total | P value |
|-----------------|-------------------------|------|-------|------------|
| | Low | High | | |
| Stage | | | | 2.9494e-03 |
| Stage I | 176 | 197 | 373 | |
| Stage II | 40 | 40 | 80 | |
| Stage III | 54 | 101 | 155 | |
| Stage IV | 30 | 66 | 96 | |
| Pathologic_T | | | | 4.6634e-03 |
| T1 | 191 | 206 | 397 | |
| T2 | 46 | 51 | 97 | |
| T3 | 74 | 144 | 218 | |
| T4 | 5 | 10 | 15 | |
| Pathologic_N | | | | 0.1887 |
| N0 | 106 | 171 | 277 | |
| N1 | 19 | 17 | 36 | |
| N2 | 2 | 2 | 4 | |
| N3 | 0 | 0 | 0 | |
| Pathologic_M | | | | 0.1442 |
| M0 | 179 | 294 | 473 | |
| M1 | 25 | 60 | 85 | |
| M2 | 0 | 0 | 0 | |
| M3 | 0 | 0 | 0 | |

it was revealed that high expression paired with a lower survival probability (Figure 4C). These results suggested that *MANCR* might promote the ccRCC development.

Knockdown of *MANCR* inhibited cell proliferation and promoted apoptosis of 786-O and SN12C cells

To explore the function of *MANCR* in ccRCC, lentivirus carrying shRNA of *MANCR* (shLncMANCR-1, shLncMANCR-2, and shLncMANCR-3) were prepared and used to knockdown the expression of *MANCR* in 786-O and SN12C cells. *MANCR* expression was significantly downregulated following transfection with a lentivirus containing shLncMANCR-3 of *MANCR* both in 786-O (64.8%) and SN12C cells (75.2%) than that in control group (Figure 5A). Therefore, lentivirus carrying shLncMANCR-3 was selected for further study. CCK-8 assay indicated that *MANCR* suppression greatly inhibited the proliferation of both 786-O and SN12C cells compared with the control group (Figure 5B). Colony formation assays also confirmed the results which showed significantly proliferation capacity inhibition of both 786-O and SN12C cells with *MANCR* knockdown compared with control group (Figure 5C). In contrast, flow cytometry assay showed that compared with control group the apoptosis of both 786-O and SN12C cells was significantly promoted by suppressing *MANCR* expression (Figure 5D). These results demonstrated that knockdown of *MANCR* hindered cell proliferation and promoted apoptosis of 786-O and SN12C cells.

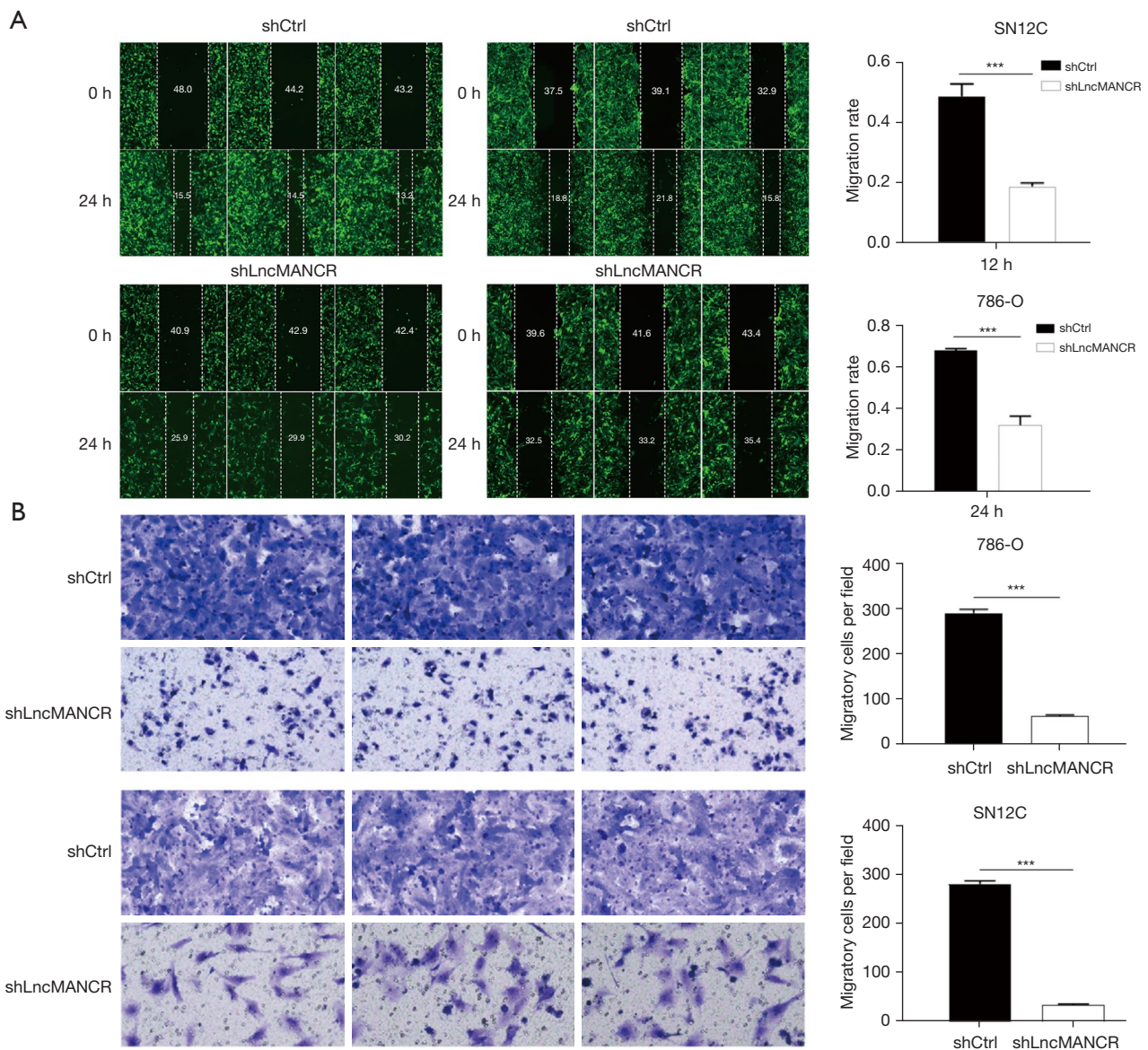


Figure 6 Knockdown of lncRNA MANCR inhibits the migration of 786-O and SN12C cells. (A) Wound healing assay was performed to detect the migration of 786-O and SN12C cells by suppressing MANCR, lentivirus carrying shLncMANCR-3 and shRNA control was transfected into cells and photographed using cellomics in a green fluorescence channel, magnification 100x. (B) Transwell assay was used to detect the migration of 786-O and SN12C cells by suppressing MANCR was detected by Transwell assay, cells were stained with 400 μ L crystal violet for 5 minutes, magnification 100x. ***, $P < 0.001$ vs. Control group. lncRNA, long non-coding RNA.

Knockdown of MANCR inhibited the migration of 786-O and SN12C cells

Subsequently, the function of MANCR on the migration of 786-O and SN12C cells was detected by both wound healing and transwell assays. The results indicated that the migration rate significantly decreased both in 786-

O and SN12C cells when suppressing MANCR compared with the control group in wound healing assay (Figure 6A). The transwell assay showed that the number of both 786-O and SN12C cells with migration dramatically decreased when suppressing MANCR than that in the control group (Figure 6B). These results indicated that knockdown of MANCR inhibited the migration of 786-O and SN12C cells.

Discussion

Currently, ccRCC is the most common pathological type of renal cell carcinoma and is mainly treated by surgery. The prognosis is poor because of most ccRCC patients have distant metastasis at the time of diagnosis. On one hand, ccRCC is insensitive to chemotherapy and radiotherapy. On the other hand, emerging treatments are currently ineffective and expensive, such as molecularly-targeted therapy and immunotherapy. Thus, it is really important to find key sensitive and specific molecular markers for the prognosis of ccRCC. Dysregulated lncRNAs have been shown to be involved in the occurrence and metastasis of tumors, suggesting that lncRNAs might be potential target for the prognosis and treatment in cancers. Therefore, it is urgent to develop a combined prognostic lncRNA signature with better performance for the prognosis of ccRCC. In the present study, a 4-lncRNAs prognostic model, which showed good performance for prognosis of ccRCC patients, was established. We demonstrated that *MANCR* was especially highly expressed in both ccRCC cells and tissues. Functionally, *MANCR* suppression inhibited cell proliferation and migration, and promoted apoptosis of 786-O and SN12C cells.

The lncRNAs participated in the processes of epigenetic, transcriptional or post-transcriptional regulation which will lead the abnormal changes for various kinds of gene expression (18). Increasing numbers of studies have shown that lncRNA play crucial roles in the development of ccRCC via regulating cell proliferation, apoptosis, invasion, and migration (19). Many lncRNA have also been shown to participate in the pathogenesis of ccRCC, including lncRNA *ADAMTS9-AS2*, lncRNA *AFAP1-AS1*, and lncRNA *Lucat1* (20-22). In addition, several lncRNAs have shown potential for prognostic assessment of ccRCC (23), such as lncRNA *OTUD6B-AS1*, lncRNA *CCAT1*, and lncRNA *SNHG17* (13,24,25). Although previous studies have attempted to analyze association between lncRNA and the prognosis of ccRCC using risk scoring models., However, most of the studies only focus on the assessment for the prognosis of ccRCC from the perspective of the unique lncRNA. Recently, Zeng *et al.* constructed a 6-lncRNA-based risk score which could be used for ccRCC prognosis based on RNA-sequencing data (26). Dou *et al.* also constructed 7-metastasis-related genes that correlated with the prognosis with the metastasis-related lncRNA signature in ccRCC (27). Su *et al.* also showed that 3-key combined lncRNA signature was successfully used to predict poor

prognosis in patients with ccRCC (28). In the present study, 1,567 differentially expressed lncRNAs in ccRCC were discerned with 1,340 upregulation and 227 downregulation. Subsequently, based on 4 lncRNA (*MANCR*, *AC018648.1*, *AC103706.1*, and *FIRRE*), was used to establish a model that was further used to The model based on multivariate Cox regression analysis indicated that the OS of low-risk patients was greatly better than that in the high-risk patients. A good performance of the model was also obtained in predicting the OS of patients with ccRCC based on the AUC of the ROC curve. The accuracy of the model was also confirmed by the C-index. These results demonstrated that the 4-lncRNA risk score showed good performance for the prognosis of ccRCC patients.

lncRNAs FIRRE and *MANCR* have been shown that they could participate in the development of cancers act as promoters. Multivariate Cox analysis in endometrial cancer patients indicated that highly *FIRRE* expression was considered as an independent risk factor for prognosis of endometrial cancer (29). Wang *et al.* showed that lncRNA *FIRRE* affected *YOD1* expression which will promote gallbladder cancer progression via sponging *miR-520a* (30). Shen *et al.* indicated that cell proliferation and glycolysis of hepatocellular carcinoma was promoted by lncRNA *FIRRE* via regulating *PFKFB4* expression (31). Liu *et al.* showed that lncRNA *FIRRE* promoted diffuse large B-cell lymphoma development by stimulating *Smurf2* decay and stabilizing B-cell receptor (32). For lncRNA *MANCR*, it has been shown that *MANCR* promoted the malignant progression of lung adenocarcinoma, esophageal carcinoma, and prostate cancer (33-35). Upregulation of *MANCR* was also considered a biomarker for poor survival predication in gastric cancer (36) and potential diagnostic marker for breast carcinoma (37). However, the function of these 2 lncRNAs in ccRCC remains unclear. In the present study, *MANCR* was showed highly expressed in ccRCC cells and tissues. Further analysis showed that high expression of *MANCR* was positively related to the stage and pathologic_T and showed a lower survival probability. In addition, we found that knockdown of *MANCR* inhibited cell proliferation and migration and promoted apoptosis of 786-O and SN12C cells. These results suggested that *MANCR* might promote ccRCC development. On the other hand, the 4-lncRNA cluster was shown to be reliable for predicting the prognosis of ccRCC patients, and providing a reference for the effective formulation of individualized treatment plans and improving prognosis of patients.

Conclusions

In summary, we established a 4-lncRNAs prognostic model which showed good performance for prognosis assessment of ccRCC patients. We also demonstrated that knockdown of *MANCR* inhibited cell proliferation and migration, and promoted apoptosis of 786-O and SN12C cells, suggesting that *MANCR* promotes ccRCC progression. This model provides a theoretical basis for the prognosis evaluation of patients with ccRCC, and *lncRNA MANCR* in the model may be a new promising target for adjuvant therapy.

Acknowledgments

Funding: This study received funding from the Key Project of Natural Science Research in Colleges and Universities of Anhui Province (No. kj2020a0557); Anhui Academic and Technical Leader Backup Candidate Project (No. 2020h213); the Key Project of Support Plan for Outstanding Young Talents in Colleges and Universities of Anhui Provincial Department of Education (No. gxyqzd2021117); and National University Student Innovation Experimental Project (No. 202010367035).

Footnote

Reporting Checklist: The authors have completed the MDAR reporting checklist. Available at <https://tau.amegroups.com/article/view/10.21037/tau-22-527/rc>

Data Sharing Statement: Available at <https://tau.amegroups.com/article/view/10.21037/tau-22-527/dss>

Conflicts of Interest: All authors have completed the ICMJE uniform disclosure form (available at <https://tau.amegroups.com/article/view/10.21037/tau-22-527/coif>). The authors have no conflicts of interest to declare.

Ethical Statement: The authors are accountable for all aspects of the work in ensuring that questions related to the accuracy or integrity of any part of the work are appropriately investigated and resolved. The study was conducted in accordance with the Declaration of Helsinki (as revised in 2013).

Open Access Statement: This is an Open Access article distributed in accordance with the Creative Commons

Attribution-NonCommercial-NoDerivs 4.0 International License (CC BY-NC-ND 4.0), which permits the non-commercial replication and distribution of the article with the strict proviso that no changes or edits are made and the original work is properly cited (including links to both the formal publication through the relevant DOI and the license). See: <https://creativecommons.org/licenses/by-nc-nd/4.0/>.

References

- Jonasch E, Walker CL, Rathmell WK. Clear cell renal cell carcinoma ontogeny and mechanisms of lethality. *Nat Rev Nephrol* 2021;17:245-61.
- Wolf MM, Kimryn Rathmell W, Beckermann KE. Modeling clear cell renal cell carcinoma and therapeutic implications. *Oncogene* 2020;39:3413-26.
- Atkins MB, Tannir NM. Current and emerging therapies for first-line treatment of metastatic clear cell renal cell carcinoma. *Cancer Treat Rev* 2018;70:127-37.
- Xie L, Li H, Zhang L, et al. Autophagy-related gene P4HB: a novel diagnosis and prognosis marker for kidney renal clear cell carcinoma. *Aging (Albany NY)* 2020;12:1828-42.
- Li D, Liu S, Xu J, et al. Ferroptosis-related gene CHAC1 is a valid indicator for the poor prognosis of kidney renal clear cell carcinoma. *J Cell Mol Med* 2021;25:3610-21.
- Zhang Y, Chen M, Liu M, et al. Glycolysis-Related Genes Serve as Potential Prognostic Biomarkers in Clear Cell Renal Cell Carcinoma. *Oxid Med Cell Longev* 2021;2021:6699808.
- Quinn JJ, Chang HY. Unique features of long non-coding RNA biogenesis and function. *Nat Rev Genet* 2016;17:47-62.
- Chan JJ, Tay Y. Noncoding RNA:RNA Regulatory Networks in Cancer. *Int J Mol Sci* 2018;19:1310.
- Na XY, Hu XQ, Zhao Y, et al. LncRNA DNAJC3-AS1 functions as oncogene in renal cell carcinoma via regulation of the miR-27a-3p/PRDM14 axis. *Eur Rev Med Pharmacol Sci* 2021;25:1291-301.
- Liu Y, Li X, Zhang C, et al. LINC00973 is involved in cancer immune suppression through positive regulation of Siglec-15 in clear-cell renal cell carcinoma. *Cancer Sci* 2020;111:3693-704.
- Liu SB, Wang HF, Xie QP, et al. LncRNA SNHG16 promotes migration and invasion through suppression of CDKN1A in clear cell renal cell carcinoma. *Eur Rev Med*

- Pharmacol Sci 2020;24:7216.
12. Cox A, Tolkach Y, Kristiansen G, et al. The lncRNA Fer1L4 is an adverse prognostic parameter in clear-cell renal-cell carcinoma. *Clin Transl Oncol* 2020;22:1524-31.
 13. Wu J, Dong G, Liu T, et al. LncRNA SNHG17 promotes tumor progression and predicts poor survival in human renal cell carcinoma via sponging miR-328-3p. *Aging (Albany NY)* 2021;13:21232-50.
 14. Zhang S, Zhang F, Niu Y, et al. Aberration of lncRNA LINC00460 is a Promising Prognosis Factor and Associated with Progression of Clear Cell Renal Cell Carcinoma. *Cancer Manag Res* 2021;13:6489-97.
 15. Cui T, Guo J, Sun Z. A computational prognostic model of lncRNA signature for clear cell renal cell carcinoma with genome instability. *Expert Rev Mol Diagn* 2022;22:213-22.
 16. Qu L, Wang ZL, Chen Q, et al. Prognostic Value of a Long Non-coding RNA Signature in Localized Clear Cell Renal Cell Carcinoma. *Eur Urol* 2018;74:756-63.
 17. Xuan Y, Chen W, Liu K, et al. A Risk Signature with Autophagy-Related Long Noncoding RNAs for Predicting the Prognosis of Clear Cell Renal Cell Carcinoma: Based on the TCGA Database and Bioinformatics. *Dis Markers* 2021;2021:8849977.
 18. Peng WX, Koirala P, Mo YY. LncRNA-mediated regulation of cell signaling in cancer. *Oncogene* 2017;36:5661-7.
 19. Zhang H, Yu L, Chen J, et al. Role of Metabolic Reprogramming of Long non-coding RNA in Clear Cell Renal Cell Carcinoma. *J Cancer* 2022;13:691-705.
 20. Song EL, Xing L, Wang L, et al. LncRNA ADAMTS9-AS2 inhibits cell proliferation and decreases chemoresistance in clear cell renal cell carcinoma via the miR-27a-3p/FOXO1 axis. *Aging (Albany NY)* 2019;11:5705-25.
 21. Mu Z, Dong D, Wei N, et al. Silencing of lncRNA AFAP1-AS1 Inhibits Cell Growth and Metastasis in Clear Cell Renal Cell Carcinoma. *Oncol Res* 2019;27:653-61.
 22. Xiao H, Bao L, Xiao W, et al. Long non-coding RNA Lucat1 is a poor prognostic factor and demonstrates malignant biological behavior in clear cell renal cell carcinoma. *Oncotarget* 2017;8:113622-34.
 23. Wu H, Wu H, Sun P, et al. Effect of Aberrant Long Noncoding RNA on the Prognosis of Clear Cell Renal Cell Carcinoma. *Comput Math Methods Med* 2021;2021:6533049.
 24. Wang G, Zhang ZJ, Jian WG, et al. Novel long noncoding RNA OTUD6B-AS1 indicates poor prognosis and inhibits clear cell renal cell carcinoma proliferation via the Wnt/ β -catenin signaling pathway. *Mol Cancer* 2019;18:15.
 25. Jing J, Zhao X, Wang J, et al. Potential diagnostic and prognostic value and regulatory relationship of long noncoding RNA CCAT1 and miR-130a-3p in clear cell renal cell carcinoma. *Cancer Cell Int* 2021;21:68.
 26. Zeng JH, Lu W, Liang L, et al. Prognosis of clear cell renal cell carcinoma (ccRCC) based on a six-lncRNA-based risk score: an investigation based on RNA-sequencing data. *J Transl Med* 2019;17:281.
 27. Dou Q, Gao S, Gan H, et al. A Metastasis-Related lncRNA Signature Correlates With the Prognosis in Clear Cell Renal Cell Carcinoma. *Front Oncol* 2021;11:692535.
 28. Su Y, Zhang T, Tang J, et al. Construction of Competitive Endogenous RNA Network and Verification of 3-Key lncRNA Signature Associated With Distant Metastasis and Poor Prognosis in Patients With Clear Cell Renal Cell Carcinoma. *Front Oncol* 2021;11:640150.
 29. Wang X, Dai C, Ye M, et al. Prognostic value of an autophagy-related long-noncoding-RNA signature for endometrial cancer. *Aging (Albany NY)* 2021;13:5104-19.
 30. Wang S, Wang Y, Wang S, et al. Long Non-coding RNA FIRRE Acts as a miR-520a-3p Sponge to Promote Gallbladder Cancer Progression via Mediating YOD1 Expression. *Front Genet* 2021;12:674653.
 31. Shen C, Ding L, Mo H, et al. Long noncoding RNA FIRRE contributes to the proliferation and glycolysis of hepatocellular carcinoma cells by enhancing PFKFB4 expression. *J Cancer* 2021;12:4099-108.
 32. Liu QH, Dai GR, Wu Y, et al. LncRNA FIRRE stimulates PTBP1-induced Smurf2 decay, stabilizes B-cell receptor, and promotes the development of diffuse large B-cell lymphoma. *Hematol Oncol* 2022. [Epub ahead of print]. doi: 10.1002/hon.3004.
 33. Liu C, Li H, Li X, et al. LncRNA MANCR positively affects the malignant progression of lung adenocarcinoma. *BMC Pulm Med* 2021;21:272.
 34. Fan J, Wang F. MANCR drives esophageal carcinoma progression by targeting PDE4D. *J BUON* 2021;26:1517-22.
 35. Nagasawa M, Tomimatsu K, Terada K, et al. Long non-coding RNA MANCR is a target of BET bromodomain protein BRD4 and plays a critical role in cellular migration and invasion abilities of prostate cancer. *Biochem Biophys*

- Res Commun 2020;526:128-34.
36. Yao L, Yan J, Gan L, et al. Upregulation of MANCR predicts poor survival in patients with gastric cancer. *Oncol Lett* 2019;18:6801-6.
37. Tahmouresi F, Razmara E, Pakravan K, et al. Upregulation of the long noncoding RNAs DSCAM-AS1 and MANCR is a potential diagnostic marker for breast carcinoma. *Biotechnol Appl Biochem* 2021;68:1250-6.

Cite this article as: Xue S, Guo H, Wei S, Song Y, Huang J, Deng S, Li Q, Li W. Identification of a combined lncRNA prognostic signature and knockdown of lncRNA MANCR to inhibit progression of clear cell renal cell carcinoma by bioinformatics analysis. *Transl Androl Urol* 2022;11(9):1304-1317. doi: 10.21037/tau-22-527